AIAA JOURNAL
Vol. 33, No. 7, July 1995

# Power Flow and Consumption in Piezoelectrically Actuated Structures

Su-Wei Zhou* and Craig A. Rogers†
*Virginia Polytechnic Institute and State University, Blacksburg, Virginia 24061*

**In a piezoelectric (PZT) actuator-driven adaptive structure, the electromechanical power consumption and power flow of the system are dominated by the complex electromechanical impedance of the system. The entire actuator/substrate system can essentially be represented by a coupled electromechanical system model. This paper presents such a system model to quantitatively determine where the energy goes and how the power is consumed in an active structure. The formulation of a coupled electromechanical admittance for a generic PZT actuator-driven two-dimensional structure was developed. The model was then used to predict the power factor, the power dissipation, and the power requirement of the system. As a numerical example, the modeling approach was applied to a simply supported thin plate excited by a pair of PZT path actuators in pure bending mode. A parametric study was performed to examine the nature and components of electromechanical power flow and consumption in the active structure. An experiment was conducted to directly measure the complex electromechanical admittance of an integrated PZT/plate system to verify the theoretical model.**

## Nomenclature

$a$ = length of structure
$b$ = width of structure
$d$ = piezoelectric constant
$E$ = electric field
$F$ = force output of piezoelectric actuator
$H$ = mechanical admittance
$h$ = thickness of structure
$I$ = current
$i$ = imaginary part of a complex number
$k$ = wave number
$P$ = dissipative power
$Q$ = reactive power
$t$ = time
$u$ = displacement in $x$ direction
$V$ = voltage
$v$ = displacement in $y$ direction
$S$ = Young's modulus
$Y$ = electromechanical admittance
$Z$ = mechanical impedance
$W$ = complex power
$\delta$ = dielectric loss factor
$\varepsilon$ = strain
$\eta$ = structural loss factor
$\nu$ = Poisson's ratio
$\rho$ = mass density
$\sigma$ = stress
$\omega$ = angular frequency

*Superscript*

$*$ = complex parameter

*Subscripts*

$p$ = parameters of piezoelectric actuator
$x$ = $x$ direction
$y$ = $y$ direction
0 = magnitude of electrical parameters
1, 2, 3 = piezoelectric material directions

Received Feb. 26, 1994; revision received Sept. 19, 1994; accepted for publication Sept. 20, 1994. 

*Ph.D. Research Associate, Mechanical Engineering, Center for Intelligent Material Systems and Structures. Member AIAA.

†Professor and Director, Mechanical Engineering, Center for Intelligent Material Systems and Structures. Member AIAA.

## Introduction

PIEZOELECTRIC (PZT) materials have been widely used as actuators and sensors in active structural vibration and acoustic control because of their compact size and good dynamic performance.[1–3] A great deal of effort has focused on the analysis and optimization of the mechanical performance of PZT transducers.[1–8] However, investigations of the power consumption and electrodynamics of PZT actuator-driven adaptive structures have been limited. There appears to be little in the literature on the topic of power relations for active structures. In fact, adaptive structures are complex electromechanical coupling systems in which electrical energy is converted into mechanical energy and vice versa. The ability and efficiency of the energy conversion of the actuators is always of concern in the design and application of active structures, especially for aerospace applications. Large and complex aerospace structures may require a great number of relatively large actuators, which will dictate large, expensive power supplies. Thus, minimizing the power consumption and enhancing the energy conversion efficiency of actuators will result in reductions in the cost and mass of the system, two of the major objectives in designing intelligent structures.[9] To achieve this, it is highly desirable to explore the nature and components of electromechanical power flow and consumption in active structures.

Liang et al.[10] suggested a coupled electromechanical analysis for a piezoelectric actuator-driven spring-mass-damper system and discussed the concepts of actuator power factor and energy transfer of the system. Lomenzo et al.[11] developed a technique to maximize mechanical power transfer from stacked PZT actuators to host structures. Hagood et al.[2] proposed a dynamic model to include the coupling between the actuator, structure, and electrical network. The model is based on a finite element analysis using the Rayleigh–Ritz energy formulation. However, his work does not discuss electromechanical power relations in active structures, and the actuator force loading is not explicitly expressed as a function of the input impedance of the actuator itself and the mechanical impedance of the host structure. A mechanical impedance model applicable to two-dimensional structures[7–8] focused on quantifying the mechanical outputs of PZT actuators; and this model now needs to be extended to include system electrical parameters to analyze electromechanical power flow and consumption in PZT actuator-driven active structures.

The concept of energy conversion in a PZT actuator-driven system involves a two-step conversion: one is the energy transfer from the support power electronics to the integrated PZT/substrate mechanical system; the other is the energy conversion from the electrical energy of the PZT actuator to the mechanical energy driving the host structure. The focus of this current work is on the analysis of the second-step energy conversion, i.e., the electromechanical power consumption and power flow in PZT actuator-driven active structures. In this paper, the formulation of a coupled electromechanical admittance for generic two-dimensional PZT actuator-driven structures will be derived. The model will be used to analyze the components of the electromechanical power flow, and to determine the power consumption and energy conversion efficiency of an integrated PZT/plate system. A parametric study will examine the effects of different system elements on power dissipation and energy transfer, including the effects of damping and geometric parameters. An experiment on a simply supported thin plate using an impedance analyzer will be conducted so that the theoretical model can be validated.

## Coupled Electromechanical System Model

A schematic of a two-dimensional PZT/substrate coupling system is shown in Fig. 1. The PZT element is used as an actuator to excite the host structure. It is assumed that the integrated system is linear, and the host structure is a generic two-dimensional structure. The host structural dynamics are represented by the direct impedance $Z_{xx}$ and $Z_{yy}$, and the cross impedance $Z_{xy}$ and $Z_{yx}$, as shown in Fig. 1. When a voltage is applied to the piezoelectric patches along the polarization direction (3), an in-plane strain is induced in the PZT actuator in both the $x(1)$ and $y(2)$ directions. This induced strain applies active forces ($F_x$ and $F_y$) on the host structure. Thus, only the in-plane motion of the actuator is considered in the following development of formulations. Furthermore, it is assumed that the PZT material is isotropic, which results in $d_{31} = d_{32}$. The in-plane motion of the actuator is similar to an equivalent thermal expansion or contraction occurring in both $x$ and $y$ directions. The equation of motion of the PZT actuator, derived from Newton's law of motion and strain-displacement compatibility, may be expressed by

$$\rho_p \frac{\partial^2 u}{\partial t^2} = S_p^* \frac{\partial^2 u}{\partial x^2} \tag{1a}$$

$$\rho_p \frac{\partial^2 v}{\partial t^2} = S_p^* \frac{\partial^2 v}{\partial y^2} \tag{1b}$$

where $S_p^*$ is the Complex Young's modulus at a zero electrical field

$$S_p^* = S_p(1 + i\eta_p) \tag{2}$$

The sinusoidal time response of the PZT actuator can be solved from Eq. (1),

$$u = [A \sin(k_{p11}x) + B \cos(k_{p11}x)]e^{i\omega t} \tag{3a}$$

$$v = [C \sin(k_{p22}y) + D \cos(k_{p22}y)]e^{i\omega t} \tag{3b}$$

where $A$, $B$, $C$, and $D$ are unknowns and can be determined by the boundary conditions; and the wave number is expressed by

$$k_p = k_{p11} = k_{p22} = \omega\sqrt{\rho_p / S_p^*} \tag{4}$$

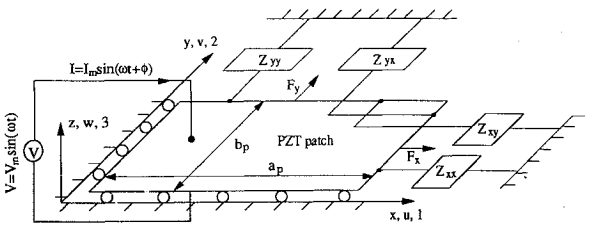


**Fig. 1 Coupled electromechanical model of a two-dimensional integrated PZT/substrate system.**

Applying the equivalent displacement boundary conditions $u_{x=0} = 0$ and $v_{y=0} = 0$, as shown in Fig. 1, to Eq. (3), the response of the PZT actuator is reduced to

$$u = A \sin(k_p x)e^{j\omega t} \tag{5a}$$

$$v = C \sin(k_p y)e^{j\omega t} \tag{5b}$$

The unknowns $A$ and $C$ may be evaluated from the constitutive equation of the PZT material at $x = a_p$ and $y = b_p$

$$\begin{pmatrix} \varepsilon_x \\ \varepsilon_y \end{pmatrix} = \begin{pmatrix} \dfrac{\partial u}{\partial x} \\ \dfrac{\partial v}{\partial y} \end{pmatrix} = \frac{1}{S_p^*}\begin{pmatrix} 1 & -\nu_p \\ -\nu_p & 1 \end{pmatrix}\begin{pmatrix} \sigma_x \\ \sigma_y \end{pmatrix} + \begin{pmatrix} d_{31} \\ d_{32} \end{pmatrix} E \tag{6}$$

where $d_{31}$ and $d_{32}$ are the piezoelectric constants of the PZT material in the 1 and 2 directions, respectively. The force outputs of the PZT actuator, $F_x$ and $F_y$, are equal and opposite to the reactions of the host structure. The induced stress at the edge of the PZT patch $\sigma_{x(y)}$ may be expressed using the mechanical impedance of the host structure

$$\begin{pmatrix} \sigma_x \\ \sigma_y \end{pmatrix} = -\begin{pmatrix} 1/(b_p h_p) & 0 \\ 0 & 1/(a_p h_p) \end{pmatrix}\begin{pmatrix} Z_{xx} & Z_{xy} \\ Z_{yx} & Z_{yy} \end{pmatrix}\begin{pmatrix} \dot{u} \\ \dot{v} \end{pmatrix} \tag{7}$$

Substituting Eqs. (5) and (7) into Eq. (6) and taking the algebraic operation to rearrange $A$ and $C$ yields

$$\begin{bmatrix} k_p C_a\left(1 - \nu_p \dfrac{b_p Z_{yx}}{a_p Z_{pxx}} + \dfrac{Z_{xx}}{Z_{pxx}}\right) & k_p C_b\left(\dfrac{a_p Z_{xy}}{b_p Z_{pyy}} - \nu_p \dfrac{Z_{yy}}{Z_{pyy}}\right) \\ k_p C_a\left(\dfrac{b_p Z_{xy}}{a_p Z_{pxx}} - \nu_p \dfrac{Z_{xx}}{Z_{pxx}}\right) & k_p C_b\left(1 - \nu_p \dfrac{a_p Z_{yx}}{b_p Z_{pyy}} + \dfrac{Z_{yy}}{Z_{pyy}}\right) \end{bmatrix}\begin{pmatrix} A \\ C \end{pmatrix} = \begin{pmatrix} d_{31} \\ d_{32} \end{pmatrix} E \tag{8}$$

where $C_a = \cos(k_p a_p)$ and $C_b = \cos(k_p b_p)$. $Z_{pxx}$ and $Z_{pyy}$ are the input mechanical impedance of the PZT actuator in the $x$ and $y$ directions, defined as

$$Z_{pxx} = \frac{F_x}{\dot{u}} = -i\frac{S_p^* h_p}{\omega}\frac{k_p b_p}{\tan(k_p a_p)} \tag{8a}$$

$$Z_{pyy} = \frac{F_y}{\dot{v}} = -i\frac{S_p^* h_p}{\omega}\frac{k_p a_p}{\tan(k_p b_p)} \tag{8b}$$

Solving the unknowns $A$ and $C$ from Eq. (8) leads to

$$\begin{pmatrix} A \\ C \end{pmatrix} = [M]^{-1}\begin{pmatrix} d_{31} \\ d_{32} \end{pmatrix} E \tag{9}$$

where $[M]$ is the coefficient matrix of $A$ and $C$ in Eq. (8). Substituting Eqs. (5) and (10) into Eq. (7), the dynamic stress output of the PZT actuator is then determined by

$$\begin{pmatrix} \sigma_x \\ \sigma_y \end{pmatrix} = \frac{S_p^* E}{1 - \nu_p^2}\begin{pmatrix} 1 & \nu_p \\ \nu_p & 1 \end{pmatrix}\left[k_p\begin{pmatrix} \cos(k_p x) & 0 \\ 0 & \cos(k_p y) \end{pmatrix} \times [M]^{-1}\begin{pmatrix} d_{31} \\ d_{32} \end{pmatrix} - \begin{pmatrix} d_{31} \\ d_{32} \end{pmatrix}\right] \tag{11}$$

The constitutive equation of the PZT material is again invoked in terms of the electrical displacement field $D_3$ in the $z(3)$ direction[6]

$$D_3 = \varepsilon_{33}^* E + d_{31}\sigma_x + d_{32}\sigma_y \tag{12}$$

where

$$\varepsilon_{33}^* = \varepsilon_{33}(1 - i\delta_p) \tag{13}$$

is the complex dielectric constant at a constant stress. Substituting Eq. (11) into Eq. (12) and letting $d_{32} = d_{31}$ yields the electrical displacement field

$$D_3 = E\left\{\varepsilon_{33}^* + \frac{d_{31}^2 S_p^*}{1-\nu_p}\left(k_p[\cos(k_p x)\cos(k_p y)] \times [M]^{-1}\begin{pmatrix}1\\1\end{pmatrix} - 2\right)\right\} \tag{14}$$

where the applied electric field $E$ can be expressed in terms of the applied voltage $V$

$$E = \frac{V}{h_p} = \frac{V_0}{h_p}e^{i\omega t} \tag{15}$$

The charge in the PZT patch can be obtained by integrating the displacement in Eq. (14) with respect to $x$ and $y$

$$q = \int_0^{a_p}\int_0^{b_p} D_3\,dx dy \tag{16}$$

The current is thus given by

$$I = I_0 e^{i\omega t} = \dot{q} = iV_0\omega\frac{a_p b_p}{h_p}\left\{\varepsilon_{33}^* - \frac{2d_{31}^2 S_p^*}{1-\nu_p} + \frac{d_{31}^2 S_p^*}{1-\nu_p}\begin{bmatrix}\frac{s_1}{a_p} & \frac{s_2}{b_p}\end{bmatrix} \times [M]^{-1}\begin{pmatrix}1\\1\end{pmatrix}\right\}e^{i\omega t} \tag{17}$$

where $s_1 = \sin(k_p a_p)$ and $s_2 = \sin(k_p b_p)$. When the PZT actuator is driven by an active voltage $V$, the current in the circuit $I$ is related to the driven voltage through the coupled electromechanical admittance, $Y^* = I/V$. Accordingly, rewriting Eq. (17) produces the coupled electromechanical admittance

$$Y^* = i\omega\frac{a_p b_p}{h_p}\left\{\varepsilon_{33}^* - \frac{2d_{31}^2 S_p^*}{1-\nu_p} + \frac{d_{31}^2 S_p^*}{1-\nu_p} \times \begin{bmatrix}\frac{s_1}{a_p} & \frac{s_2}{b_p}\end{bmatrix}[M]^{-1}\begin{pmatrix}1\\1\end{pmatrix}\right\} \tag{18}$$

It is noted that the admittance $Y^*$ represents the integrated electromechanical characteristics of a piezoelectric actuator-driven system, and it is frequency dependent. The complex admittance $Y^*$ contains all of the parameters concerning the system electrodynamics performance, including mass, stiffness, damping, material and physical properties, electrical parameters, and boundary conditions. Once these parameters are selected, the admittance will be determined. The input structural impedance of the PZT actuator is given by Eq. (9). The mechanical impedance matrix of the host structure in Eq. (7) is determined by

$$Z = \begin{pmatrix}Z_{xx} & Z_{xy}\\ Z_{yx} & Z_{yy}\end{pmatrix} = \begin{pmatrix}H_{xx} & H_{yx}\\ H_{xy} & H_{yy}\end{pmatrix}^{-1} \tag{19}$$

where $H_{xx}$ and $H_{yy}$ are the direct mechanical admittances of the host structure at the edge of the PZT patches, and $H_{xy}$ and $H_{yx}$ are the cross mechanical admittances.

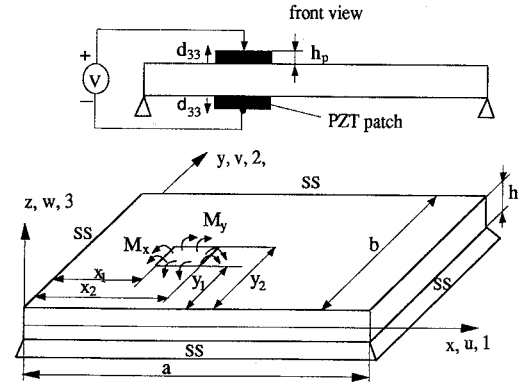


**Fig. 2 Geometry of a surface-bonded PZT actuator-driven simply supported (SS) plate.**

As an example, we consider a simply supported thin plate, as shown in Fig. 2. Two PZT actuators are assumed perfectly bonded on the top and bottom surfaces. When a voltage is applied to the PZT patches along the polarization direction 3, the PZT actuators can be actuated out-of-phase. This actuation creates two pairs of line bending moments at the boundaries of the PZT patch. Under the actuation of the line moments, an analytical solution of the mechanical admittance matrix of a simply supported plate at the mid point of the edge of the PZT patch was derived by the authors.[8] results were

$$H_{xx} = i\frac{2\pi(h+h_p)^2\omega}{\rho h a^3 b_p} \times \sum_{m=1}^{\infty}\sum_{n=1}^{\infty}\left(\frac{m^2 C_x^2 C_y \sin[n\pi(y_1+y_2)/(2b)]}{n\left(\omega_{mn}^2 - \omega^2\right)}\right) \tag{20}$$

$$H_{yy} = i\frac{2\pi(h+h_p)^2\omega}{\rho h a^3 a_p} \times \sum_{m=1}^{\infty}\sum_{n=1}^{\infty}\left(\frac{n^2 C_x C_y^2 \sin[m\pi(x_1+x_2)/(2a)]}{m\left(\omega_{mn}^2 - \omega^2\right)}\right) \tag{21}$$

$$H_{xy} = H_{yx} = i\frac{2\pi(h+h_p)^2\omega}{\rho h a^2 b b_p} \times \sum_{m=1}^{\infty}\sum_{n=1}^{\infty}\left(\frac{mC_x C_y^2 \sin[m\pi(x_1+x_2)/(2a)]}{\omega_{mn}^2 - \omega^2}\right) \tag{22}$$

where $C_x = \cos(m\pi x_1/a) - \cos(m\pi x_2/a)$ and $C_y = \cos(m\pi y_1/b) - \cos(m\pi y_2/b)$. As illustrated in Fig. 2, $x_1$, $x_2$, $y_1$, and $y_2$ are the location coordinates of the edges of the PZT patches on the plate. The resonant frequency of the plate $\omega_{mn}$ can be determined from the homogeneous equation of the transverse motion of the plate; and $m$ and $n$ are the modal indices in the $x$ and $y$ directions, respectively.

It is noted that the structural admittance is a function of driving point location on the structure, and the admittance along the edge of the PZT patch is different. The numerical calculations have shown that the midpoint admittance is a very good approximation of the average admittance along the edge of the path. For simplification and not losing generality, the admittance at the midpoint of the edge of the PZT patch is used to represent the admittance characteristics of the plate, as expressed in Eqs. (20–22).

Once the mechanical admittance (impedance) is obtained, the coupled electromechanical admittance of an integrated PZT/substrate system can be determined from Eq. (18). The electromechanical power consumption and flow of the system can then be predicted, which will be developed later.

So far, the assumption made in the derivation is that the system is linear, and the host structure is a generic two-dimensional structure. The formulation Eq. (18) is a generic solution for coupled admittance of a system and can be applied to general

two-dimensional structures. For complex structures with irregular geometry, Eq. (18) is still applicable, although a close-form solution of the structural impedance is difficult to obtain. In this case, the structural impedance can be determined from either finite element analysis or experiments.

## Electromechanical Power Consumption and Power Flow

Since a PZT actuator acts as a plate capacitor, when a voltage $V = V_0 e^{i\omega t}$ is applied to it, the current in the circuit can be expressed by

$$I = I_0 e^{i(\omega t+\phi)} \tag{23}$$

where $\phi$ is the phase between the current and voltage. The electrical power supplied to the PZT actuator is actually decomposed into two components $P$ and $Q$. The real (dissipative) power is

$$P = \frac{I_0 V_0}{2}\cos\phi = \frac{V_0^2}{2}\mathrm{Re}(Y^*) \tag{24}$$

where $\cos\phi$ is called the power factor. The reactive power is

$$Q = \frac{I_0 V_0}{2}\sin\phi = \frac{V_0^2}{2}\mathrm{Im}(Y^*) \tag{25}$$

Physically, the real power is the electrical power supplied to the PZT actuator and converted into mechanical power to drive the host structure. The reactive power is the power circulating between the electrical power source and the integrated PZT/structure system. The total power may be expressed as

$$W^* = P + iQ \tag{26}$$

The magnitude of the complex power is defined as the apparent power,

$$W_0 = \sqrt{P^2 + Q^2} = \frac{I_0 V_0}{2} = \frac{V_0^2}{2} Y_0 \tag{27}$$

where $Y_0$ is the magnitude of the admittance $Y^*$. The apparent power reflects the power requirement of the system which includes both the dissipative power and the reactive power. The emphasis of the current work is on the analysis of the dissipative power consumption of a PZT actuator-driven structure. When power supplies are considered in the system modeling, the reactive power in the system will exert an important influence on the power requirement. In that case, a large reactive power is usually expected as a high-current demand is required from the power supply. In addition, the dissipative power consumed in the power supply itself should also be considered in the power requirement for the integrated system as a whole. Future work will include the electronics of power supplies in order to determine the overall power requirement.

Substituting Eq. (27) into Eq. (24), the power factor is rewritten as

$$FP = \cos\phi = \frac{\mathrm{Re}(Y^*)}{Y_0} = \frac{P}{W_0} \tag{28}$$

The power factor FP is the ratio of the dissipative power to the apparent power and represents the energy conversion efficiency from electrical power to mechanical power in the integrated PZT/substrate system. It is noted that the dissipative power consumption, the power requirement, and the energy conversion efficiency of the system are strongly related to the coupled electromechanical admittance $Y^*$.

The dissipative (real) power in an integrated PZT/substrate system includes three parts:

The first is the power dissipated by the structural damping of the host structure, which is related to the structural loss factor $\eta$ in the complex Young's modulus. This power is proportional to the mechanical vibration power of the host structure. Second is the power consumed by the structural damping of the PZT actuator, which is associated with the mechanical loss factor $\eta_p$ of the PZT actuator. Third is the power consumption caused by the dielectric loss of the PZT actuator, which is related to the dielectric loss factor $\delta_p$ in the complex dielectric constant.

The real power is eventually converted into internal heat in the system, resulting in heat generation and inducing thermal stress in the PZT actuator.[12] The first two parts of the system power consumption just mentioned are directly used in driving the host structure. They may be considered to represent the total mechanical power dissipation in the system. A suggested actuator power factor $PF_a$ is defined as[10]

$$PF_a = \frac{\text{dissipative mechanical power}}{\text{apparent power}} = \frac{\mathrm{Re}(Y_a^*)}{|Y_a^*|}, \tag{29}$$

in which $Y_a^*$ is calculated by assuming the dielectric loss factor $\delta_p$ to be zero in Eq. (18). Apparently, the difference between the system power factor [Eq. (28)] and the actuator power factor [Eq. (29)] is that the former includes the dielectric power consumption of the PZT actuator in the dissipative power consumption. When the power factor is experimentally determined, the system power factor should be used because the dielectric loss of the PZT actuator is usually not zero in a real system. In this paper, the system power factor is used in the following numerical examples. A comparison between the system power factor and the actuator power factor will also be performed.

## Parametric Study and Discussion

A parametric study is conducted in this section to quantitatively examine how the dissipative power is consumed in the system and how much power is required to drive the system. The influence of the thickness and the location of the PZT actuator is also discussed.

A thin plate made of aluminum is used in the numerical example. The size of the plate is $304.8 \times 203.2 \times 1.53$ mm. Two PZT actuators are symmetrically bonded on the plate and located at $x_1 = 50.8$ mm and $y_1 = 25.4$ mm, as shown in Fig. 2. The size of the PZT patch is $50.8 \times 50.8 \times 0.19$ mm. The PZT material is G1195. The basic material properties are listed in Table 1. It is assumed in the numerical case that the magnitude of the voltage applied to the PZT actuator is 20 V.

Figure 3 illustrates the components and distribution of the dissipative (real) power in the frequency domain. The solid line represents the total dissipative power. The dashed line is the power consumption of the mechanically loss of the plate obtained from Eq. (24) by assuming $\delta_p = \eta_p = 0$. The dash-dotted line is the power consumption from the mechanical loss of the PZT actuator, found by setting $\delta_p = \eta = 0$ in Eq. (24). The dotted line is the power consumed by the dielectric loss of the PZT actuator, found by assuming $\eta = \eta_p = 0$ in Eq. (24).

It is clearly seen in Fig. 3 that at the resonant frequencies, the dissipative power is primarily consumed by the structural damping of the plate, whereas at off resonance, it is significantly affected by the dielectric loss of the PZT itself. The mechanical damping of the PZT actuator, however, has a slight influence on the real power consumption because of its small size.

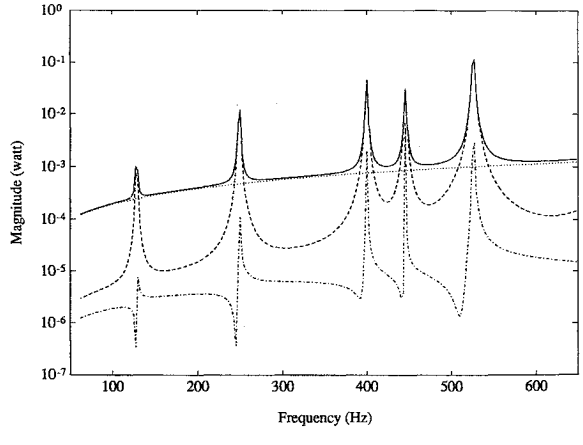


**Fig. 3 Dissipative power of an integrated PZT/substrate system: —— total dissipative power of PZT/plate system; - - - - mechanical power consumption (plate); · · · · · · mechanical power consumption (PZT); ..... dielectric power consumption (PZT).**

**Table 1 Material properties of the PZT and the aluminum**

| | Young's modulus, $N/m^2$ | Mass density $kg/m^3$ | Poisson ratio | Piezoelectric constants, m/V | Dielectric constant, F/m | Dielectric loss | Loss factor |
|---|---|---|---|---|---|---|---|
| PZT | $6.3 \times 10^{10}$ | 7650 | 0.3 | $-1.66 \times 10^{-10}$ | $1.5 \times 10^{-8}$ | 0.015 | 0.005 |
| Aluminum | $6.9 \times 10^{10}$ | 2700 | 0.33 | N/A | N/A | N/A | 0.005 |

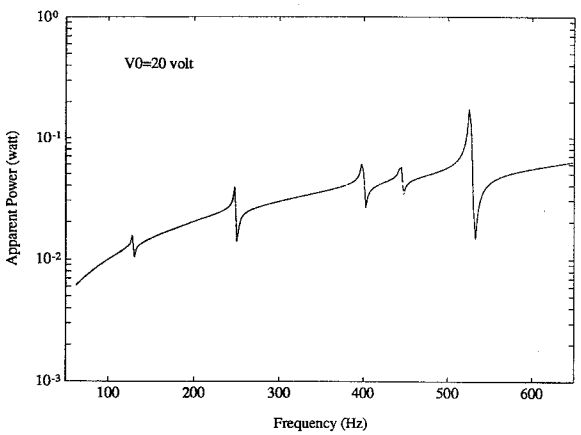


**Fig. 4 Apparent power of a PZT/plate system.**

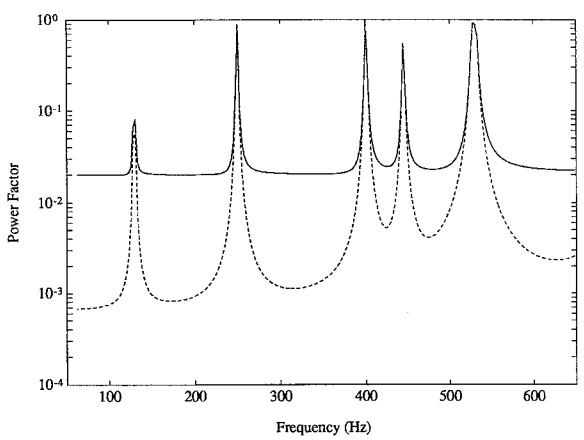


**Fig. 5 Comparison of system power factor and actuator power factor: —— system power factor; - - - - actuator power factor.**

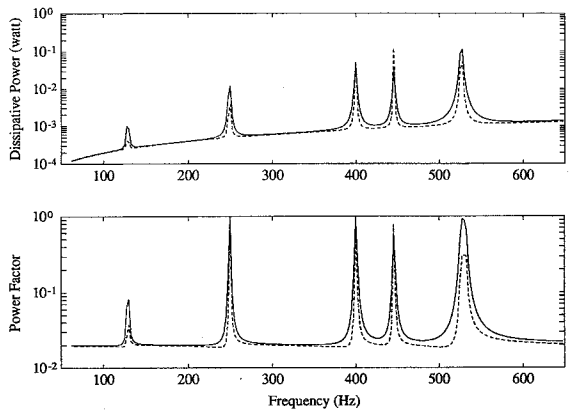


**Fig. 6 Influence of the plate loss factor on the dissipative power and power factor of a PZT/plate system:—— loss factor of plate: 0.005; - - - - loss factor of plate: 0.001.**

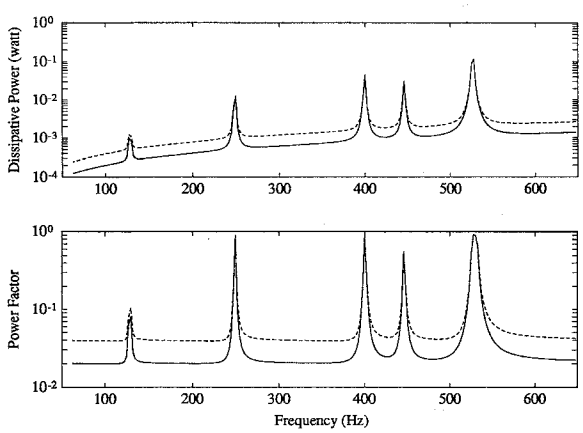


**Fig. 7 Influence of the PZT actuator dielectric loss factor on the dissipative power and power factor of a PZT/plate system: —— dielectric loss factor of PZT: 0.015; - - - - dielectric loss factor of PZT: 0.03.**

Figure 4 shows the characteristics of the apparent power of the system. The peak power appears at the fifth mode in the range of less than 650 Hz, and it can be used to estimate the power requirement of the system in this frequency band. The power consumption significantly goes up when the excitation frequency increases. Once the interesting frequency band is determined, the power requirement of the system can be numerically predicted.

Figure 5 demonstrates the difference of the power factor predicted from Eq. (28) and Eq. (29), respectively. At resonant frequencies, the power factor is maximized because of the minimum resistance to the structural vibration. Both the system power factor and the actuator power factor give the same prediction. At off resonance, however, the actuator power factor is much smaller than the system power factor because the dissipative power is dominated by the dielectric loss behavior of the PZT actuator. Assuming a zero dielectric loss gives a very low-power consumption, resulting in a low-actuator power factor.

When the damping value in the system changes, the basic relations of the power consumption as shown in Fig. 3 are still applicable. Figure 6 illustrates that if the loss factor of the plate increases from 0.001 to 0.005, the dissipative power goes up at resonant frequencies and increases slightly at off resonance. In contrast, Fig. 7 shows that if the dielectric loss factor of the PZT actuator doubles from 0.015 to 0.03, the dissipative power and the power factor increase by about 50% at off-resonant frequencies and remain the same at the resonant frequencies.

The geometric parameters of the PZT actuator, such as the thickness and the location, have significant influence on the dissipative power and the power factor because the mechanical impedance of the system strongly varies with these geometric parameters.[7,8] Under the assumption of the constant magnitude of the applied voltage ($v_0 = 20$ V), when the thickness of the PZT patch increases from 0.19 mm to $2 \times 0.19$ mm and $4 \times 0.19$ mm, the real power consumption decreases on the whole frequency band, as displayed in Fig. 8. The power factor also decreases at off resonance. However, the power factor has a complicated variation at the resonant frequencies. The observation indicates that when the thickness of the PZT actuator varies, the maximum power factor will depend on the individual mode. Another important observation in Fig. 8 is that the resonant frequencies of the system apparently shift to higher values when the thickness of the PZT actuator increases. It can be explained that the added PZT patches stiffen the original plate and shift the resonant frequencies to the high values.

Figure 9 shows that when the location of the PZT actuator on the structure varies, the mechanical impedance changes and so does

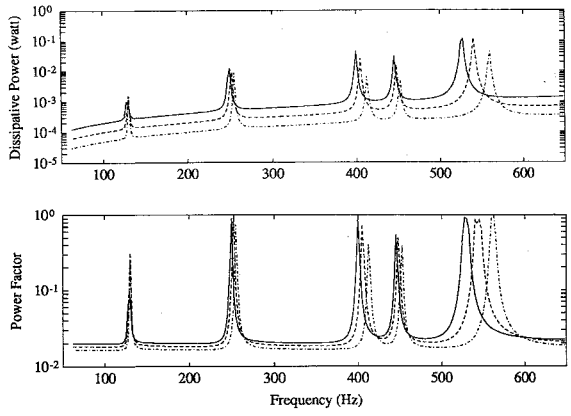


**Fig. 8 Influence of the PZT thickness on the dissipative power and power factor of a PZT/plate system: —— hp = 0.19 mm; - - - - hp = 0.38 mm; ····· hp = 0.76 mm.**

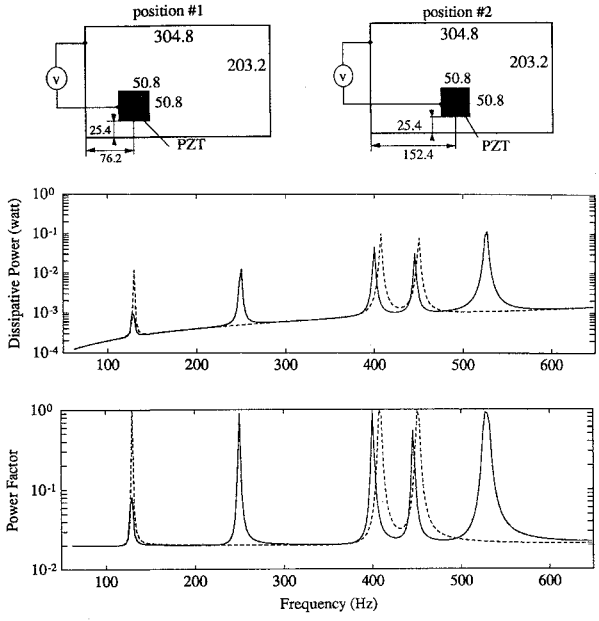


**Fig. 9 Influence of the PZT location on the dissipative power and power factor of a PZT/plate system: —— location #1; - - - - location #2.**

the power consumption of the system. Note that when the center of the PZT actuator locates at the node line position in the $x$ direction (location 2), the corresponding modes, i.e., the second and the fifth modes, are tailored off since little mechanical vibrational energy is supplied to these vibrational modes.

## Experimental Verification

A simply supported thin plate integrated with surface-bonded PZT patches was built and tested to validate the coupled electromechanical system model. The size and physical properties of the plate and the PZT material are the same as those used in the numerical calculation in the previous section. An HP 4194A impedance/gain-phase analyzer was used to directly measure the coupled electromechanical admittance of the piezoelectric actuator-driven plate. Then, a comparison between the theoretical model and the experimental results was performed.

Figure 10 illustrates the measured and predicted complex admittance of the system in terms of the real part and the imaginary part, respectively. The corresponding power factor, calculated from the experimental data using Eq. (28), is displayed in Fig. 11. In both figures, the theoretical prediction based on the complex system impedance (dashed line) agrees well with the experimental data (solid line). The coupled electromechanical system model has provided a reasonably accurate prediction of the power consumption and the energy conversion efficiency of the PZT actuator-driven

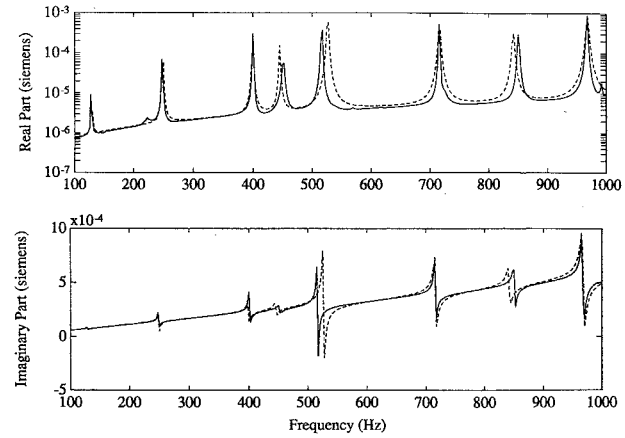


**Fig. 10 Measured and predicted complex electromechanical admittance of a PZT/plate system: ____ experimental data; _ _ _ coupled impedance model.**

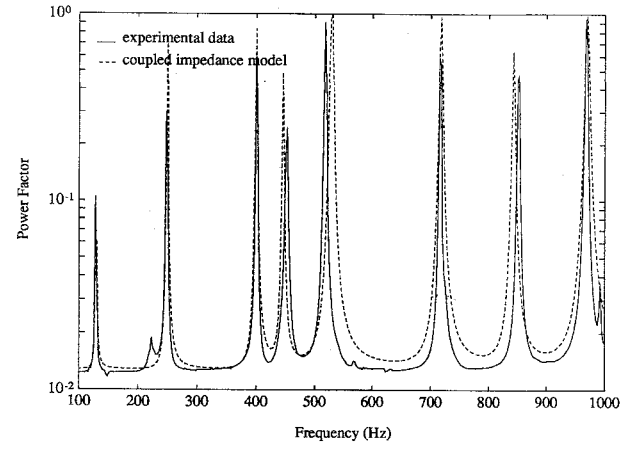


**Fig. 11 Measured and predicted power factor of a PZT/plate system.**

system. It should be noted that the maximum difference between the theoretical model and the experimental results appears at the fifth mode, i.e., (2, 2) mode. It may be explained that when the geometric center of the PZT actuator locates on the antinode position of the host plate ($x = 76.2$ mm, $y = 50.8$ mm), the excitation of that mode is maximized. The inertial effect caused by the added mass loading of the PZT patch is then intensified. The measured resonant frequency and the response of this mode [the fifth mode (2, 2)] are thus smaller than those predicted by the theoretical model.

## Summary

A coupled electromechanical system model for a generic two-dimensional piezoelectric actuator-driven structure has been developed to predict the electromechanical power consumption and power flow. This modeling approach is helpful in understanding where the energy goes and in designing induced strain actuators and energy-efficient intelligent structures.

The coupled electro-mechanical system model has been experimentally verified.

The parametric study has demonstrated that the dissipative power supplied to the PZT actuator is primarily consumed by the mechanical damping of the host structure at resonant frequencies and is dissipated by the dielectric loss of the PZT itself at off resonance.

The thickness and location of the PZT actuator have an impact on the dissipative power consumption and power factor of the integrated system because these geometric parameters may cause significant changes in the mechanical impedance of the system.

Future work on system power consumption will include the electronics of power supplies in order to determine the overall power requirement. Additional work will also focus on power flow relations under closed-loop control.

## Acknowledgments

The authors gratefully acknowledge the support of the Air Force Office of Scientific Research under AFOSR Grant F49620-93-1-0166; C. I. Chang, Program Manager.

## References

[1]Dimitriadis, E. K., Fuller, C. R., and Rogers, C. A., "Piezoelectric Actuators for Distributed Noise and Vibration Excitation of Thin Plates," *Proceedings of the 8th Biennial Conference on Failure Prevention and Reliability*, American Society of Mechanical Engineers, Montreal, Canada, DE-Vol. 16, Sept. 1989, pp. 223–233.

[2]Hagood, N. M., Chung, W. H., and von Flotow, A., "Modeling of Piezoelectric Actuator Dynamics for Active Structural Control," *Proceedings of the AIAA/ASME/ASCE/AHS/ASC 31st Structures, Structural Dynamics, and Materials Conference* (Long Beach, CA), AIAA, Washington, DC, 1990, pp. 2242–2256 (AIAA Paper 90-1097).

[3]Wang, B. T., "Active Control of Sound Transmission/Radiation from Elastic Plates Using Multiple Piezoelectric Actuators," Ph.D. Dissertation, Dept. of Mechanical Engineering, Virginia Polytechnic Inst. and State Univ., Blacksburg, VA, June 1991.

[4]Crawley, E. F., and Lazarus, K. B., "Induced Strain Actuation of Isotropic and Anisotropic Plates," *AIAA Journal*, Vol. 29, No. 6, 1991, pp. 945–951.

[5]Crawley, E. F., and de Luis, J., "Use of Piezoelectric Actuators as Elements of Intelligent Structures," *AIAA Journal*, Vol. 25, No. 10, 1987, pp. 1373–1385.

[6]Ikeda, T., *Fundamentals of Piezoelectricity*, Oxford Univ. Press, New York, 1990.

[7]Zhou, S. W., Liang, C., and Rogers, C. A., "Impedance Modeling of Two-Dimensional Piezoelectric Actuators Bonded on a Cylinder," *Proceedings of the Adaptive Structures and Material Systems*, American Society of Mechanical Engineers, Winter Annual Meeting, New Orleans, LA, 1993, pp. 247–256.

[8]Zhou, S. W., Liang, C., and Rogers, C. A., "A Dynamic Model of Piezoelectric Actuator-Driven Thin Plates," *Proceedings of Smart Structures and Materials*, Society of Photo-Optical Instrumentation Engineers, Orlando, FL, 1994, Vol. 2190, pp. 550–562.

[9]Rogers, C. A., "Intelligent Material Systems: The Dawn of a New Materials Age," *Journal of Intelligent Material Systems and Structures*, Vol. 4, No. 1, 1993, pp. 4–12.

[10]Liang, C., Sun, F. P., and Rogers, C. A., "Coupled Electro-Mechanical Analysis of Piezoelectric Ceramic Actuator-Driven Systems—Determination of the Actuator Power Consumption and System Energy Transfer," *Proceedings of Smart Structures and Materials*, Society of Photo-Optical Instrumentation Engineers, Albuquerque, NM, 1993, pp. 229–235.

[11]Lomenzo, R. A., Sumali, H., and Cudney, H. H., "Maximizing Mechanical Power Transfer from Piezoelectric Stacked Actuators to Structures," *Proceedings of the Adaptive Structures and Material Systems*, American Society of Mechanical Engineers, Winter Annual Meeting, New Orleans, LA, 1993, pp. 229–235.

[12]Zhou, S. W., Liang, C., and Rogers, C. A., "Temperature Rise and Thermal Stress of Piezoelectric Elements in Active Structures," *Proceedings of the Adaptive Structures and Material Systems*, American Society of Mechanical Engineers International Mechanical Engineering Congress and Exposition, Chicago, IL, 1994, American Society of Mechanical Engineers, AD-Vol. 45, MD-Vol. 54, pp. 183–191.